

A novel demodulation method for transmission using nitrogen–vacancy-based solid-state quantum sensor

Ruixin Bai(白瑞昕)1, Xinyue Zhu(朱欣岳)2, Fan Yang(杨帆)3,Tianran Gao(高天然)1, Ziran Wang(汪子然)1, Linyan Yu(虞林嫣)1,Jinfeng Wang(汪晋锋)2, Li Zhou(周力)1, and Guanxiang Du(杜关祥)1;†

Citation: Chin. Phys. B, 2022, 31 (**7**): 074203. DOI: 10.1088/1674-1056/ /ac5618
Journal homepage: http://cpb.iphy.ac.cn; http://iopscience.iop.org/cpb

What follows is a list of articles you may be interested in

Quantum key distribution transmitter chip based on hybrid-integration of silica and lithium niobates

Xiao Li(李骁), Liang-Liang Wang(王亮亮), Jia-shun Zhang(张家顺), Wei Chen(陈巍), Yue Wang(王玥), Dan Wu (吴丹), and Jun-Ming An (安俊明)
Chin. Phys. B, 2022, 31 (**6**): 064212. DOI: 10.1088/1674-1056/ac40fe

Nonlocal nonreciprocal optomechanical circulator

Ji-Hui Zheng(郑继会), Rui Peng(彭蕊), Jiong Cheng(程泂), Jing An(安静), and Wen-Zhao Zhang(张闻钊)
Chin. Phys. B, 2022, 31 (**5**): 054204. DOI: 10.1088/1674-1056/ac4100

Quantum storage of single photons with unknown arrival time and pulse shapes

Yu You(由玉), Gong-Wei Lin(林功伟), Ling-Juan Feng(封玲娟), Yue-Ping Niu(钮月萍), and Shang-Qing Gong(龚尚庆)
Chin. Phys. B, 2021, 30 (**8**): 084207. DOI: 10.1088/1674-1056/abfbd3

Speeding up generation of photon Fock state in a superconducting circuit via counterdiabatic driving

Xin-Ping Dong(董新平), Xiao-Jing Lu(路晓静), Ming Li(李明), Zheng-Yin Zhao(赵正印), and Zhi-Bo Feng(冯志波)
Chin. Phys. B, 2021, 30 (**4**): 044214. DOI: 10.1088/1674-1056/abe297

Dissipative quantum phase transition in a biased Tavis-Cummings model

Zhen Chen(陈臻), Yueyin Qiu(邱岳寅), Guo-Qiang Zhang(张国强), Jian-Qiang You(游建强)
Chin. Phys. B, 2020, 29 (**4**): 044201. DOI: 10.1088/1674-1056/ab7b55

RAPID COMMUNICATION

A novel demodulation method for transmission using nitrogen–vacancy-based solid-state quantum sensor

Ruixin Bai(白瑞昕)[1], Xinyue Zhu(朱欣岳)[2], Fan Yang(杨帆)[3], Tianran Gao(高天然)[1], Ziran Wang(汪子然)[1], Linyan Yu(虞林嫣)[1], Jinfeng Wang(汪晋锋)[2], Li Zhou(周力)[1], and Guanxiang Du(杜关祥)[1,†]

[1] *College of Telecommunication & Information Engineering, Nanjing University of Posts and Telecommunications, Nanjing* 210000, *China*
[2] *College of Electronic and Optical Engineering, Nanjing University of Posts and Telecommunications, Nanjing* 210000, *China*
[3] *College of Automation & College of Artificial Intelligence, Nanjing University of Posts and Telecommunications, Nanjing* 210000, *China*

(Received 21 November 2021; revised manuscript received 7 February 2022; accepted manuscript online 17 February 2022)

Diamond based quantum sensing is a fast-emerging field with both scientific and technological significance. The nitrogen–vacancy (NV) center, a crystal defect in diamond, has become a unique object for microwave sensing applications due to its excellent stability, long spin coherence time, and optical properties at ambient condition. In this work, we use diamond NV center as atomic receiver to demodulate on–off keying (OOK) signal transmitted in broad frequency range (2 GHz–14 GHz in a portable benchtop setup). We proposed a unique algorithm of voltage discrimination and demonstrated audio signal transceiving with fidelity above 99%. This diamond receiver is attached to the end of a tapered fiber, having all optic nature, which will find important applications in data transmission tasks under extreme conditions such as strong electromagnetic interference, high temperatures, and high corrosion.

Keywords: NV center, demodulate OOK signal, high-frequency range, audio signal transceiving

PACS: 42.50.Ex, 07.55.Ge, 03.65.Yz **DOI:** 10.1088/1674-1056/ac5618

1. Introduction

With the development of communication technology, the common 2.4-GHz and 5-GHz electromagnetic wave signals have become the mainstream wireless fidelity (WiFi) and bluetooth communication frequency bands. Since the transmission of high-frequency electromagnetic waves can greatly increase the rate of information transmission, communications in higher frequency bands will be widely used in 5G and even 6G communications.[1–3] Nowadays, the difficulty of demodulating higher frequency signals (greater than 30 GHz) seems to be one of the key factors restricting the further development of communication technology.[4,5] A component of the demodulated signal is the band-pass filter whose performance[6–9] directly determines the quality of the communication and the signal-to-noise ratio. Nowadays, high-frequency band-pass filters mainly include surface acoustic wave (SAW)[10,11] and bulk acoustic wave (BAW)[12–14] filters, and the filters that can be used for high-frequency mobile communications are mainly BAW filters. At present, BAW filters on the market are mainly monopolized by Qorvo and Broadcom, and the bandwidth of existing band-pass filters is generally greater than 20 MHz, especially high-frequency band-pass filters, so the communication quality will be much lower than that of low-frequency transmission with narrower pass band width. The NV center of diamond has a stable high-frequency resonance frequency,[15,16] and the resonance frequency can be linearly adjusted by an external magnetic field,[17–19] and attenuates fast at the non-resonant frequency. It has the excellent characteristics of low passband width and is able to be a good tool for demodulating the high-frequency signal. In our experiment, we use a laser to excite the diamond and continuously collect the fluorescent signal returned by the diamond. We placed the diamond above the microwave antenna and judged whether the pulsed which modulate the microwave was low or high by comparing intensity of the fluorescence. The bandwidth of the equivalent band-pass filter obtained by using this method was lower than 8 MHz, which is much smaller than the high frequency band pass filter on the market, and the system has the characteristics of small size and large center frequency adjustment range, which is very convenient for carrier frequency switching and frequency division multiplexing. We finally used the system to successfully transmit audio signals under the condition of 2.87 GHz, thus verifying the feasibility and reliability of this new demodulation scheme.

2. System structure and theory

As shown in Fig. 1(a), the communication system consists of a data acquisition (DAQ) card installed in a computer, a pulse signal generator, laser, fiber diamond probe, avalanche photo diode (APD), microwave source and an antenna. We

†Corresponding author. E-mail: duguanxiang@njupt.edu.cn

© 2022 Chinese Physical Society and IOP Publishing Ltd

use a pulse signal generator to generate pulse signals in order to modulate the microwave source. We use APD to collect the fluorescent signal emitted by the diamond micro-crystal through the optical fiber. The output of APD is acquired by a data acquisition card and the computer judge the original signal through the measurement of the change of fluorescence intensity. We use a standard antenna powered by the microwave source to simulate a receiver and the fiber diamond probe is closely placed on top of the antenna. We used a permanent magnet to split all eight resonance peaks of the optically detected magnetic resonance (ODMR) curve which will be shown in Fig. 1(b) and change the frequency of the peaks by changing the strength of the magnetic field so that the communication system will be able to work at any frequencies.

2.1. The physical principle of the demodulator

The NV center is a point defect structure in diamond consisting of a substituted nitrogen atom and a nearby lattice vacancy. In quantum regulation studies, a negatively charged NV center (NV^-) is generally considered, whose vacancy provides four unpaired bonded electrons, plus one electron contributed by the nitrogen atom and one additional captured electron, and this system can be considered as an electron spin with a total spin of 1.

The NV central spin ground state is a spin triplet state with a zero-field splitting between $m_s = \pm 1$ and $m_s = 0$ at 2.87 GHz, which is in the microwave band. The $m_s = \pm 1$ state of the electron spin is 30% weaker than the $m_s = 0$ state, so the 532-nm laser is used to polarize the NV center to the $m_s = 0$ state, then the quantum state is manipulated by pulsed microwaves, and finally the current quantum state of the NV center is determined by counting the fluorescent photons.[15,16,20]

Noteworthy, when the microwave pulse is far from the resonant frequency, the laser polarizes the electrons to a state where $m_s = 0$. The fluorescence is strong and stable; when the microwave pulse is close to the operating frequency, there is a certain probability that the electrons will be flipped to a state where $m_s = \pm 1$, resulting in a decrease in fluorescence intensity.

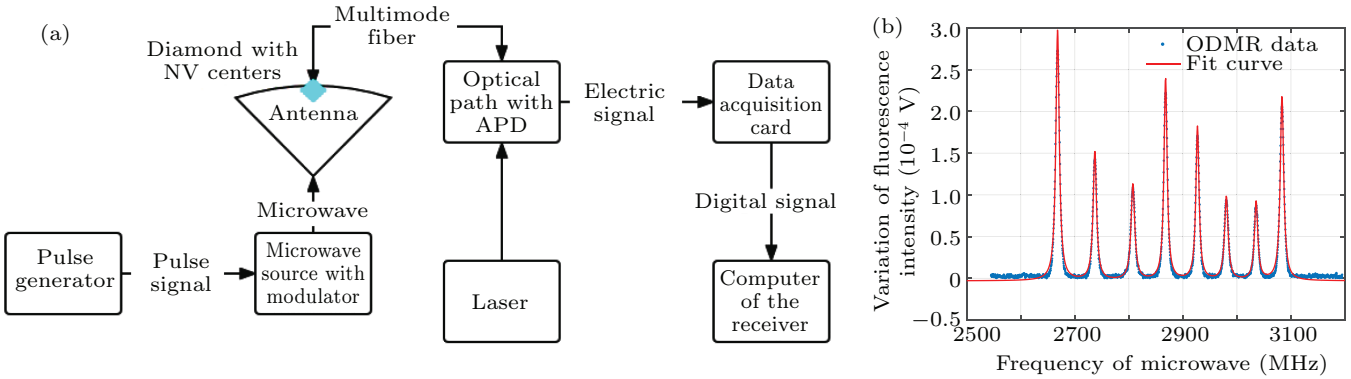


Fig. 1. (a) The schematic diagram of the setup. (b) The ODMR spectrum of the NV center and the curve fitted by Lorenz function.

As shown in Fig. 1(b), which depicts the relationship between the degree of influence on the fluorescence intensity and the microwave frequency. Since the NV axis of diamond has four directions, there will be 8 peaks at different resonant frequencies. The 8 peaks in Fig. 1(b) represent 8 resonant frequencies. The peak positions are fitted by the Lorenz function, and we get the full width at half maximum of each peak is 3.7 MHz, which means that when the frequency of the microwave is 1.85 MHz higher than the resonance frequency, the change of the obtained fluorescence intensity affected by the microwave will be sharply reduced. Thus, when the modulation pulse is at a high level, the fluorescence intensity received by us will become smaller due to the effect of microwaves at the resonance frequency. When the modulated pulse is at a low level, since there is no external microwave effect, the fluorescence intensity will not be affected. And when the electromagnetic wave we receive is not at the resonance frequency, the fluorescence intensity will not be affected. Therefore, the bandwidth of the demodulator based on the diamond NV center we designed is within the half-width (3.7 MHz), which is much smaller than the BAW filter on the market. So the communication quality it brings will theoretically be higher.

2.2. The frequency range and frequency division multiplexing

Because the demodulation bandwidth is very small, it is much more suitable for frequency division multiplexing systems. Due to the Zeeman splitting effect,[21] when a magnetic field is applied to the diamond, energy level splitting will occur, which will shift the resonance frequency. The 8 peaks shown in the ODMR spectrum will be split to both sides. When the direction of the magnetic field is perpendicular to the NV axis, the number of peaks in the ODMR spectrum will reduce to four.[18,19] As the magnetic field strength increases, the peak position, that is, the resonance frequency, will linearly increase, as shown in Fig. 2(a). Therefore, we

can easily adjust the demodulation frequency of the system through simply increasing the strength of the external magnetic field, which means that the same system can demodulate the waveform of each frequency so that the flexibility of our system is much better than the BAW in the market whose center frequency cannot change easily. And since the resonate frequency can now be pushed up to 14 GHz by increasing the magnetic field strength, our demodulation frequency adjustment range is much larger than the filter realized by using resistive devices.

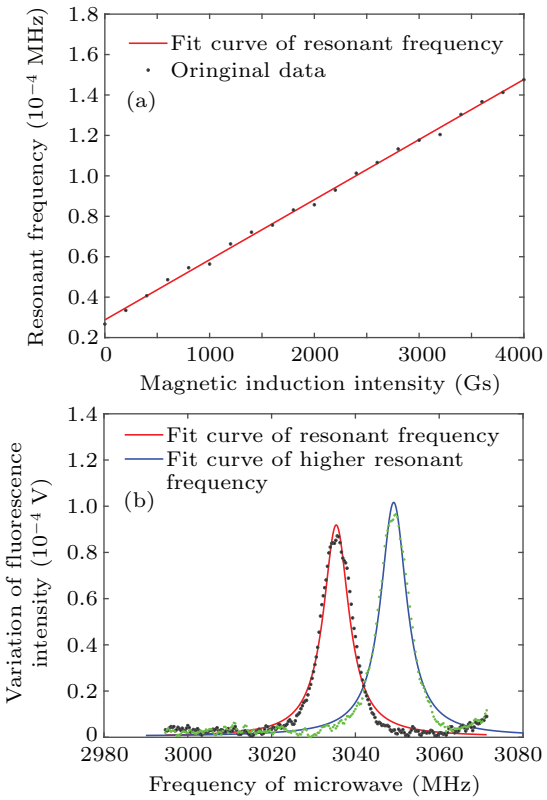


Fig. 2. (a) The relationship between magnetic field intensity and resonant frequency and (b) the shift of a single peak with slight increasement on magnetic field intensity. The unit 1 Gs = 10^{-4} T.

As shown in Fig. 2(b), the red line in the figure shows that the resonance frequency of a diamond influenced by a magnetic field is 3.035 GHz, which means that the signal with a carrier frequency of 3.035 GHz can be demodulated. The blue line in the figure indicates that the diamond is influenced by a stronger magnetic field, which makes the resonance frequency increase to 3.049 GHz. It is obvious that there is almost no overlap between the two peaks. Therefore, in theory, if two diamond samples are used simultaneously and different magnetic fields are applied to them, they will not affect each other. In this way, we are able to make full use of the spectrum.

3. Experiments and evaluation

In order to verify the feasibility of the demodulation scheme based on the NV center, we encode a segment of audio signal, converting it into a pulse sequence and modulate it with microwave source to transmit it through an antenna. For the receiver, we use 12-micron diameter diamond crystals fixed to the tip of a fiber in our experiments and bring the diamond close to the end of the receiving antenna. We set the pulse width of the microwave (MW) to 1000 ns and the output RF power to 20 dBm at microwave high levels. Microstrip antennas resonating at around 2.87 GHz are connected to microwave sources to generate microwave fields. The 532-nm constant wave (CW) laser is applied to the fiber optic probe containing NV center diamond with the microwave simultaneously, and the output power is 100 mW. We send a trigger signal to the data acquisition card at the first pulse of the microwave signal to start data collection. Figure 3 shows the scatter plot of the original signal, the timing of the smoothed signal with a window size of 20-Gs and 50-Gs smoothing and the discriminated output pulse signal.

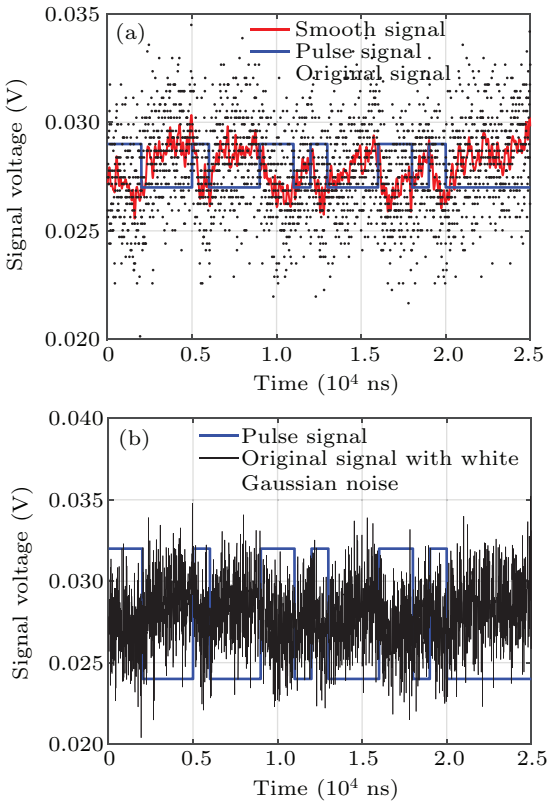


Fig. 3. (a) Comparation of the original signal, smooth signal, and the output pulse signal with voltage discrimination algorithm. (b) Fluorescent signal with Gaussian noise and output pulse signal.

In this experiment, the sampling rate of the DAQ card is 100 MHz, which means that one hundred points are collected for each 1000-ns pulse. The sampling depth is 16 bits, we set the range to ±5 V, and the sampling accuracy is about 15 mV, so the vertical distribution of the data points in Fig. 3. has a more obvious step-like character. In order to reduce the bit error ratio (BER), we uniquely take into account the effect of the delay in the rising edge of the fluorescence signal intensity on the discrimination by incorporating a judgement of the fluorescence signal trend into the algorithm and using iterations to

find the optimal threshold. Then we found that the BER could also be reduced by encoding the audio into repeated binary sequences, enabling the data collector to repeatedly and continuously capture and poll the switching information for the same timing pulses. In the end, we added Gaussian noise to the raw data to check the robustness of the transmission system and algorithm. Comparison of signals with and without noise is shown in the figure and table.

In Table 1, we compare the effect of different sampling rates and number of repetitions on the BER and transmission rate (TR). We show that repeated transmissions of the same pulse sequence are discriminated independently and the results are voted on, with the higher the number of repetitions, the higher the BER and the corresponding decrease in transmission rate. As shown in the first column of Table 1, our BER can be as low as 0.66% and our transmission rate can be up to 2266.96 bit/s, at two different repetitions.

Table 1. Results of transmission evaluation. In the table, T is the number of repetitions; Time is the total transmission time of the 5010 binary bits(s); BER is the bit error rate, which is the number of error bits/total number of bits transmitted; TR is the transmission rate.

T	Time	BER (%)	BER with noise (%)	TR (bit/s)
1	2.21	8.06	8.46	2266.96
3	5.14	3.14	3.39	974.71
7	18.50	0.66	0.66	270.81

4. Conclusion and perspectives

We developed a special communication system to demodulate the OOK signal by a diamond quantum receiver and attempt to transmit the audio signal. Then we used a unique algorithm of voltage discrimination due to the delay of the demodulation, which greatly reduce the BER compared to direct averaging of the sampled voltage of the pulse. The sampling rate in this work is 100 MHz and the rise time is around 1000 ns, which is limited by the relatively weak microwave field and can be significantly shorter with higher power transmission. The fall time is limited to the decay rate of intersystem crossing (ISC), which is on the order of $\sim$ 250 ns.

In an unpublished work, we have explored the way in which general audio signals other than music audio signals are transmitted in this system. Because of the problem of accumulated heat inside the diamond when using continuous wave laser, the transmission rate and the bit error rate might be improved by optimizing the power of laser. What is more, adjusting the decision threshold in real time might be another method to reduce the bit error rate. We also intend to further explore the possibility of applying our system in the domain of transmitting other kinds of signals and using frequency division multiplexing in practice.

Acknowledgement

Project supported by the National Key Research and Development Program of China (Grant No. 2021YFB2012600).

References

[1] Li Y, Gao B, Zhang X and Huang K 2020 *IEEE Access* **8** 13282
[2] Rappaport T S, Sun S, Mayzus R, Zhao H, Azar Y, Wang K, Wong G N, Schulz J K, Samimi M and Gutierrez F 2013 *IEEE Access* **1** 335
[3] Roh W, Seol J Y, Park J, Lee B, Lee J, Kim Y, Cho J, Cheun K and Aryanfar F 2014 *IEEE Commun. Mag.* **52** 106
[4] Uwaechia A N and Mahyuddin N M 2020 *IEEE Access* **8** 62367
[5] Al-Ogaili F and Shubair R M 2016 *proceedings of the* 2016 *IEEE International Symposium on Antennas and Propagation (APSURSI)*, 1003
[6] Zhong Y, Yang Y, Zhu X, Dutkiewicz E, Shum K M and Xue Q 2017 *IEEE Electron Dev. Lett.* **38** 626
[7] Guo Y J, Da Xu K, Liu Y and Tang X 2018 *IEEE Access* **6** 10249
[8] Shaman H and Hong J S 2007 *IEEE Microwave Wireless Components Letters* **17** 193
[9] Jung S and Yang S I 2010 *Proceedings of the* 2010 *Asia-Pacific Microwave Conference*, 1059
[10] Novgorodov V, Freisleben S, Hornsteiner J, Schmachtl M, Vorotnikov B, Heide P and Vossiek M 2009 *Proceedings of the* 2009 *Asia Pacific Microwave Conference*, 2072
[11] Takai T, Iwamoto H, Takamine Y, Yamazaki H, Fuyutsume T, Kyoya H, Nakao T, Kando H, Hiramoto M and Toi T 2016 *Proceedings of the* 2016 *IEEE International Ultrasonics Symposium (IUS)*, 1
[12] Bogner A, Bauder R, Timme H J, Reccius C, Weigel R and Hagelauer A 2019 *Proceedings of the* 2019 *IEEE International Ultrasonics Symposium (IUS)*, 1685
[13] Moe C, Olsson R, Patel P, Tang Z, D'agati M, Winters M, Vetury R and Shealy J 2020 *Proceedings of the* 2020 *IEEE International Ultrasonics Symposium (IUS)*, 1
[14] Thalhammer R, Fattinger G, Handtmann M and Marksteiner S 2006 *Proceedings of the* 2006 *IEEE MTT-S International Microwave Symposium Digest*, 390
[15] Appel P, Ganzhorn M, Neu E and Maletinsky P 2015 *New J. Phys.* **17** 112001
[16] Dong M M, Hu Z Z, Liu Y, Yang B, Wang Y J and Du G X 2018 *Appl. Phys. Lett.* **113** 131105
[17] Stepanov V, Cho F H, Abeywardana C and Takahashi S 2015 *Appl. Phys. Lett.* **106** 063111
[18] Chen G B, He W H, Dong M M, Zhao Y and Du G X 2020 *IEEE Sensors Journal* **20** 2440
[19] Chen G, Hui Y, Sun J, He W and Du G 2020 *Chin. Phys. Lett.* **37** 114203
[20] Robledo L, Bernien H, Van Der Sar T and Hanson R 2011 *New J. Phys.* **13** 025013
[21] Maekawa S and Fukuyama H 1981 *J. Phys. Soc. Jpn.* **50** 2516